

Phase matching in femtosecond BOXCARS

D. Romanov,^{1,2} A. Filin,^{1,2} R. Compton,^{1,3} and R. Levis^{1,3,*}

¹Center for Advanced Photonics Research, College of Science and Technology, Temple University, Philadelphia, Pennsylvania 19122, USA

²Department of Physics, Temple University, Philadelphia, Pennsylvania 19122, USA

³Department of Chemistry, Temple University, Philadelphia, Pennsylvania 19122, USA

*Corresponding author: rjlevis@temple.edu

Received May 22, 2007; revised August 10, 2007; accepted September 15, 2007;
posted October 1, 2007 (Doc. ID 83283); published October 24, 2007

We analytically describe the effect of phase-matching conditions on femtosecond BOXCARS line shape and demonstrate quantitative agreement with experimental spectra for the oxygen vibrational transition, $\Delta G_{01} = 1556.4 \text{ cm}^{-1}$. © 2007 Optical Society of America
OCIS codes: 190.7110, 190.4380, 190.5650.

Phase matching is an essential component for all nonlinear conversion processes and must be taken into consideration for quantitative line shape analysis. For coherent anti-Stokes Raman scattering (CARS) a maximum in the signal intensity (resonant or nonresonant) occurs when the phase-matching condition $\Delta \mathbf{k} = \mathbf{k}_{P1} + \mathbf{k}_{P2} - \mathbf{k}_S - \mathbf{k}_{CARS} = 0$ is satisfied, where \mathbf{k}_{P1} , \mathbf{k}_{P2} , \mathbf{k}_S , and \mathbf{k}_{CARS} are the wave vectors for the two pump, Stokes, and CARS beams, respectively. The simplest means of achieving phase matching in CARS is through collinear beam geometry, with the \mathbf{k}_{CARS} photons generated in the same direction as the pump and Stokes beams. Phase-matching conditions for the collinear configuration are increasingly relaxed as the beams become more tightly focused into the sample [1]. Femtosecond CARS has been performed in the collinear configuration in (1) broadband experiments, where all beams are of fs duration [2], and (2) multiplex experiments, where only the Stokes beam is typically of fs duration [3–6]. The principle drawback to collinear CARS is the necessity to filter the output signal, a point that becomes especially relevant in gaseous samples where concentrations are low and there is little output signal to spare. The filtering and combining (via a dichroic beam splitter) processes of the beams in the collinear geometry can cause significant loss of signal. In addition, tight focusing is often not feasible when working with vacuum chambers and/or other geometric restrictions that are commonly employed for gas-phase experiments, rendering the phase-matching conditions as less than optimal.

An elegant means of avoiding the inherent background, as well as the tight focus restriction, was developed using a BOXCARS beam geometry to impart a unique direction on \mathbf{k}_{CARS} for spatial filtering [7,8]. Long in use in the nanosecond and picosecond regimes, BOXCARS has recently become an important tool for experiments requiring fs time resolution, for instance, in measurements of temperature [9–12], rotational and vibrational constants [9,10], and wavepacket dynamics [13,14].

However, in the fs BOXCARS regime an appreciable wave-vector mismatch occurs between the various frequency components within the fs pulses due to the broad bandwidth and noncollinearities.

This necessitates a detailed analysis of the phase-matching conditions. In this Letter we present a theoretical description that accounts for the broad bandwidth of the fs pulses and the corresponding phase-matching effects on fs BOXCARS. This theory is compared with experiments on oxygen.

We will consider the phase-matching conditions for fs BOXCARS as outlined in the inset of Fig. 1. The two pump beams of frequency ω_P that impinge the focusing lens (L1) lie in the horizontal plane and are separated by a distance d ; the Stokes beam of frequency ω_S is incident at a distance h above the plane of the pump beams. Both L1 and L2 lenses have the same focal distance, f .

The finite diameter of the beams ($2r_0$) and finite duration of the pulses are two major sources of phase mismatch in fs BOXCARS. The finite diameter leads to mismatch of the directions of the participating

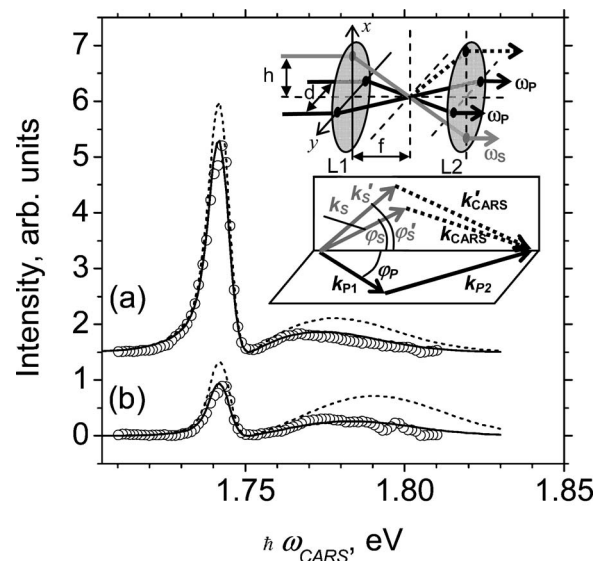


Fig. 1. Typical dependence of CARS signal intensity on CARS photon energy for two different Stokes photon energies, (a) 1.385 eV and (b) 1.401 eV, in fs BOXCARS experiment. Circles represent the experiment. Dashed curve, theory without the mismatch attenuation correction; solid curve, theory with the correction. The inset shows the beam geometry for folded BOXCARS and phase-matching conditions for fs BOXCARS (see details in the text).

wave vectors \mathbf{k}_S and \mathbf{k}'_S , as shown in the inset to Fig. 1. This detuning of the Stokes wave vector as a function of angle is $\sim r_0/h$. The finite (and short) temporal duration of the pulses leads to a relatively broad frequency distribution and thus causes considerable detuning of the wave vector magnitudes within a given laser pulse. For the same Stokes beam, this detuning is $\sim \delta\omega_S/c\omega_S$. The phase-mismatch tolerance to the frequency deviations and the corresponding phase-mismatch attenuation of the output CARS signal will be determined by the interaction length and the transverse beam profiles.

To account for CARS output signal distortion due to phase mismatching, we assume that the experimental alignment condition provides perfect phase match for infinitely narrow beams having carrier frequencies $\omega_{P1}=\omega_{P2}=\omega_{P0}$ and $\omega_S=\omega_{S0}$. This corresponds to the following relation between φ_{S0} and φ_{P0} , the angles of incidence for the excitation beams at the focal spot (see the inset of Fig. 1):

$$\tan(\varphi_{S0}) = \frac{\tan(\varphi_{P0})}{\sqrt{g}}, \quad g = \left(2\frac{\omega_{P0}}{\omega_{S0}} - 1\right)^{-1}. \quad (1)$$

Small deviations of the frequencies and the angles from their phase-matching values bring about the phase mismatch in the CARS wave vector, according to the energy and momentum conservation rules

$$\begin{aligned} \omega_{P1} + \omega_{P2} - \omega_S &= \omega_{CARS}, \\ \mathbf{k}_{P1} + \mathbf{k}_{P2} - \mathbf{k}_S &= \mathbf{k}_{CARS}. \end{aligned} \quad (2)$$

Let us assume that in the plane of the lens L1 in Fig. 1, the three beams are centered at the points satisfying the conditions of Eq. (1); the beams have transverse Gaussian shape with the same diameter $2r_0 \ll d, h$ and small frequency deviations, $\delta\omega_S = \omega_S - \omega_{S0}$, $\delta\omega_{P1} = \omega_{P1} - \omega_{P0}$, and $\delta\omega_{P2} = \omega_{P2} - \omega_{P0}$. Then, for the portions of these beams that have the local Cartesian coordinates x_i, y_i ($i=S, P1, P2$) measured from the respective beam center, the amount of the wave-vector mismatch is obtained from approximate solution of Eqs. (2) as

$$\begin{aligned} \delta k_{CARS} &= \frac{\omega_{P0} d}{c} \frac{d}{2} \left(\sqrt{g}(x_1 + x_2 - 2x_3) + (y_1 - y_2) \right. \\ &\quad \left. - \frac{d g + 1}{2} \frac{\omega_{P0}}{\omega_{S0}} \left(2\frac{\delta\omega_S}{\omega_{S0}} - \frac{\delta\omega_{P1} + \delta\omega_{P2}}{\omega_{P0}} \right) \right), \end{aligned} \quad (3)$$

to the first order of the small parameters $|x_i/f|$ and $|\delta\omega_i/\omega_{i0}|$. This correction leads to the relative suppression of the CARS output through the mismatch attenuation factor, $F(\delta\omega_{P1}, \delta\omega_{P2}, \delta\omega_S)$, produced by the averaging (over the spatial variables) of the usual factor, $\sin^2(l\delta k_{CARS})/(l\delta k_{CARS})^2$, with the Gaussian profiles of the three beams and thus determined by the interplay of the effective interaction length, l , and the transverse distribution width of the pump and Stokes beams, r_0 .

For the small-angle experiment setup considered here, l is approximately found as the intersection of the three Gaussian beams in the focal region. The sine function with the argument given by Eq. (3) is a fast-oscillating function of the variables x_1, x_2, x_3, y_1 , and y_2 on the r_0 scale; thus we can approximate the averaging integral over these variables and obtain (for $\omega_{P1}=\omega_{P2}$) the following simplified expression for the mismatch attenuation factor:

$$\begin{aligned} F(\omega_{CARS}, \omega_S) &= \frac{1}{r_0 \sqrt{2\pi(1+3g)}} \\ &\quad \times \exp\left(-\left(\frac{d}{2r_0}\right)^2 \frac{(g+1)^2}{2(1+3g)} \frac{1}{(2\omega_{P0})^2}\right. \\ &\quad \left. \times \left(\frac{\omega_S}{g} - \omega_{CARS}\right)^2\right), \end{aligned} \quad (4)$$

where d is the distance between the two pump beams on the focusing lens and g is defined by Eq. (1).

In the experimental setup, a 50 fs Ti:sapphire regenerative amplifier was used to generate pump pulses centered at 800 nm with a 425 fs pulse duration and 1 kHz repetition rate and to pump the optical parametric amplifier (OPA) generating the 140 fs Stokes pulse. The OPA was scanned to provide all the necessary Stokes frequencies. The excitation beams were focused ($f=25$ cm) into an optical chamber to measure the spectrum of oxygen (300 K, 1 atm.).

Figure 1 displays measurements of the spectrally resolved fs BOXCARS signal collected with the Stokes photon energy detuned from resonance for (a) 28 meV and (b) 44 meV (corresponding to $\hbar\omega_S = 1.385$ eV and $\hbar\omega_S = 1.401$ eV, respectively, with the resonance condition occurring at $\hbar\omega_S = \hbar\omega_{S0} = 1.357$ eV). The experimental measurements (circles) for the oxygen vibrational transition $\Delta G_{01} = 1556.4$ cm⁻¹ (that is, $\hbar\omega_{P0} - \hbar\omega_{S0} = 193$ meV) display a peak centered at $\hbar\omega_{CARS} = 1.743$ eV for the resonant signal with a spectral position independent of $\hbar\omega_{S0}$. The broad peak in each spectrum corresponds to the nonresonant contribution (with position dependent upon $\hbar\omega_{S0}$).

In a simple collinear geometry, when the mismatch attenuation is neglected, the CARS signal line shape can be described by a model analytical curve as follows. Assuming the width of the probed energy level to be much smaller than the bandwidths of the probing fs pulses, we incorporate multipath Raman processes inherent in fs CARS into the analysis of the line shape by summing over all paths contributing to a particular CARS emission frequency. Our theory results in analytical expressions for the CARS signal intensity as a function of detunings and spectral bandwidths (details will be reported elsewhere [15]). In particular, the dependence of the emitted CARS signal on the CARS and Stokes frequencies, at a fixed frequency of the pump beam, is obtained as

$$I_{\text{CARS}}(\omega_{\text{CARS}}, \omega_S) = I_0 e^{-(1+\alpha)(\omega_{\text{CARS}} + \omega_S - 2\omega_P)^2 / (2+\alpha)^2 \sigma} \times \left| \beta + i e^{-(\omega_F)^2 / 2\sigma} \right| \times \left(1 + \text{Erf} \left(\frac{i\omega_F}{\sqrt{2}\sigma} \right) \right)^2, \quad (5)$$

where $\omega_F = ((2+\alpha)\Omega + \omega_S + \alpha\omega_P - (1+\alpha)\omega_{\text{CARS}}) / (2+\alpha)$; the parameters σ and α are given by the pump and Stokes linewidths: $\sigma = (1+\alpha)(FWHM_P)^2 / ((2+\alpha)4 \ln 2)$, $\alpha = (FWHM_S / FWHM_P)^2$. In Fig. 1, the dashed curve corresponds to a fit using Eq. (5) without taking into account the mismatch attenuation that occurs for each value of Stokes photon energy. The solid curve is a fit using Eqs. (4) and (5), including the mismatch attenuation correction. Only two fitting parameters, I_0 and β , were used to create the theoretical curves. I_0 represents the maximum intensity of the CARS signal given a particular experimental arrangement, and β represents the ratio of nonresonant to resonant signal. The remaining parameters were taken from experiment. Figure 1 depicts the significant discrepancy between theory and experiment when the geometrical phase-matching condition is ignored. Without the correction, the peak in the resonant and nonresonant signal in both spectra far exceeds that in the experimental data.

Figure 2 shows the CARS spectrum of the fundamental vibrational transition of oxygen at $\Delta G_{01} = 1556.4 \text{ cm}^{-1}$. Theoretical curves were simulated using the same set of parameters as in Fig. 1. The experimental and theoretical curves were generated by integrating over the CARS photon energy (integrating the curves as depicted in Fig. 1 for all values of

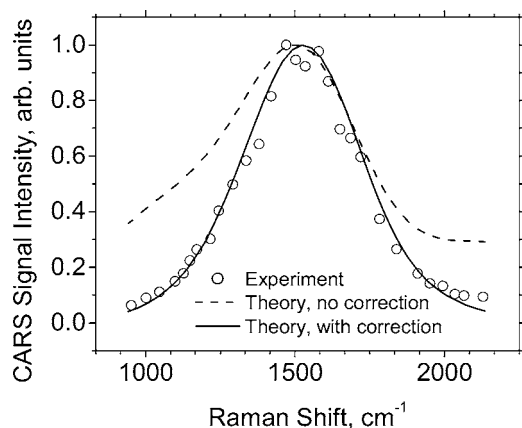


Fig. 2. Integrated CARS spectrum of the oxygen vibrational transition $\Delta G_{01} = 1556.4 \text{ cm}^{-1}$. Circles represent the experiment. Dashed curve, theory without the mismatch attenuation correction; solid curve, theory with the correction. The spectra are normalized (see details in the text)

Stokes detuning). The experimental data (circles) generate a line shape that differs significantly from what could be expected based on an intuitive picture germane to narrowband CARS. That is, the nonresonant background should not diminish to zero at large Stokes detunings, but should rather level off to some constant value that is caused by nonresonant electronic polarization and is independent of the Raman shift, according to Eq. (5). The theoretical curve without mismatch attenuation correction (dashed curve) predicts that the nonresonant contribution to the signal remains constant with large detuning. Upon application of Eq. (4), the theoretical curve (solid curve) is in excellent agreement with the experimental data.

To summarize, it has been shown that for correct analysis of the data taken in fs BOXCARS it is necessary to take into account the phase-matching conditions to accurately model both the line shape of emitted CARS signal and the CARS spectrum generated from the CARS signal as a function of Stokes wavelength. The appropriate mismatch attenuation correction was developed theoretically, and the theoretical predictions are in good agreement with experiment.

This work is supported by DARPA.

References

1. G. C. Bjorklund, *IEEE J. Quantum Electron.* **QE-11**, 287 (1975).
2. A. Zumbusch, G. R. Holtom, and X. S. Xie, *Phys. Rev. Lett.* **82**, 4142 (1999).
3. J.-X. Cheng, A. Volkmer, L. D. Book, and X. S. Xie, *J. Phys. Chem. B* **106**, 8493 (2002).
4. N. Dudovich, D. Oron, and Y. Silberberg, *J. Chem. Phys.* **118**, 9208 (2003).
5. D. Oron, N. Dudovich, and Y. Silberberg, *Phys. Rev. Lett.* **90**, 213902 (2003).
6. H. Kano and H. Hamaguchi, *Appl. Phys. Lett.* **85**, 4298 (2004).
7. A. C. Eckbreth, *Appl. Phys. Lett.* **32**, 421 (1978).
8. Y. Prior, *Appl. Opt.* **19**, 1741 (1980).
9. T. Lang, K.-L. Kompa, and M. Motzkus, *Chem. Phys. Lett.* **310**, 65 (1999).
10. P. Beaud, H.-M. Frey, T. Lang, and M. Motzkus, *Chem. Phys. Lett.* **344**, 407 (2001).
11. T. Lang and M. Motzkus, *J. Opt. Soc. Am. B* **19**, 340 (2002).
12. R. P. Lucht, S. Roy, T. R. Meyer, and J. R. Gord, *Appl. Phys. Lett.* **89**, 251112 (2006).
13. M. Schmitt, G. Knopp, A. Materny, and W. Kiefer, *Chem. Phys. Lett.* **270**, 9 (1997).
14. D. Pestov, R. K. Murawski, G. O. Ariunbold, X. Wang, M. C. Zhi, A. V. Sokolov, V. A. Sautenkov, Y. V. Rostovtsev, A. Dogariu, Y. Huang, and M. O. Scully, *Science* **316**, 265 (2007).
15. R. Compton, A. Filin, D. Romanov, and R. Levis, "Elucidating the spectral and temporal contributions from the resonant and nonresonant response to fs CARS," *J. Chem. Phys.* (to be published).